Progress In Electromagnetics Research C, Vol. 105, 35–45, 2020

High Efficiency X-Band Series-Fed Microstrip Array Antenna

M. Mohammadi Shirkolaei*

Abstract—A new class of the wideband series-fed microstrip array antenna is presented for X-band applications. A novel configuration of the reflector-slot-strip-foam-inverted patch (RSSIP) is proposed to provide high efficiency and wide operating frequency band. To improve the front to back ratio (FBR) and enhance the gain, a reflector is used. The series-fed configuration is selected for the array to simultaneously provide a very high efficiency and reduce the side lobe level. To experimentally verify the performance, a prototype of the array antenna is fabricated, and measurement is performed. This array consists of 12 sub-linear arrays with series-fed microstrip excitation. Also, each of these subarrays consists of 16 RSSIP antennas. An excellent agreement exists between measurement and simulation. The measured gain and efficiency of the fabricated antenna are 28.5 dB and 67% at 10 GHz, respectively. The measured impedance matching bandwidth ($S_{11} < -10$ dB) is 24% which confirms the wideband characteristic of the antenna. The series-fed configuration results in very low measured SLL of -24.5 dB at H-plane. The proposed 16×12 array antenna is a proper candidate for applications in MIMO systems and synthetic aperture radars (SAR).

1. INTRODUCTION

Microstrip antennas are low cost, low profile, and light-weight structures which are one of the popular and interesting radiating devices in the engineering and sciences. Alongside these advantages, these antennas have an easy fabrication process and can be easily integrated into planar microwave subsystems and circuits [1–9]. In many applications of array antenna, the cost, complexity, and size are significant and important challenges in the implementation. The mentioned advantages have made microstrip antenna as radiating elements in the array configuration. The applications of the microstrip array antenna in a radar system, satellite, and mobile communication are a confirmation of this claim.

In terms of feeding, the microstrip array antennas are classified in two categories, namely, parallel-fed and series-fed ones. One of the most important figures of merit in antenna and array design is radiation efficiency. Parallel-fed array suffers low efficiency due to dielectric and ohmic losses and the unwanted parasitic radiation of feedline [10, 11]. To mitigate this drawback, a series-fed network for a microstrip antenna array is proposed [12–18]. Series fed array antenna is classified into two categories. In the first category, the first feedline is excited and the end feedline terminated by the matched load [19]. This type of array acts similarly to a traveling wave antenna (TWA). In a similar way to TWA, the direction of the main beam is rotated by varying the frequency. This feature is not suitable for the applications which require radiated power in the specified direction. In the second category, the series-fed network is excited from the middle line. This type of feeding network results in the broadside radiation. The array with this feeding network acts as a standing wave antenna. To achieve wide operating bandwidth, aperture couple mechanism is presented.

The major challenge in a microstrip array antenna for achievement to the high efficiency is to reduce the mutual coupling effects between adjacent radiating elements constituting the array.

Received 10 June 2020, Accepted 12 August 2020, Scheduled 27 August 2020

* Corresponding author: M. Mohammadi Shirkolaei (m.mohammadi@ssau.ac.ir).

The author is with the Department of Electrical Engineering, Shahid Sattari Aeronautical University of Science and Technology, Tehran, Iran.

It has been shown that mutual coupling among neighboring radiating elements in the antenna can be improved by increasing the space between the elements, but this is at the cost of increased antenna size [20]. Many techniques have been investigated to reduce mutual coupling between elements, which include using metamaterials [21–25], metasurface [26–28], and embedded periphery slot [29]. The results show that the presence of these components close to a radiating element can affect its resonant frequency. In addition, a large surface area is required to implement these structures. In this paper to reduce mutual coupling, a defected ground structure (DGS) is used.

In this paper, a high efficacy microstrip array antenna is proposed for the X-band application. The series-fed network works based on the exciting middle line. These types of feeding provide the array with a tapered amplitude distribution which results in a significant reduction in side lobe level (SLL). A novel configuration of the reflector-slot-strip-foam-inverted patch (RSSIP) based on the defected ground mechanism is presented as radiating elements to enhance the bandwidth of the mentioned series-fed networks. Also, the physical arrangement of the proposed RSSIP provides appropriate radiation efficiency. An RSSIP antenna improves the front-to-back ratio (F/B) because of the reflector.

A prototype of an RSSIP array antenna is designed and fabricated to use in the experimental verification process. The array is made up of 12 subarrays. Each of these subarrays consists of 16 RSSIP antennas as a repetitive element. To provide an array with the tapered distribution and consequently reduce the SLL, the series-fed network is utilized by the middle line excitation mechanism. The measurement and simulation results are in excellent agreement. The measurement results show that the fabricated array has high efficiency of 67% and the peak gain of 28.5 dB. Also, the SLL of -24.5 dB and the high F/B of 29 dB are achieved by the measurement. The impedance matching bandwidth of 24% ($S_{11} < -10$ dB) is reported from the measurement which confirms the wideband characteristic of the proposed RSSIP array antenna.

2. ARRAY ANTENNA DESIGN

2.1. Antenna Element Design

In this section, the design methodology of the new class of RSSIP antenna as an element of the array is presented. The schematic of the proposed antenna is shown in Fig. 1. As shown in Fig. 1(a), the antenna consists of two substrates with an air gap instead of foam between them. The metallic patch is printed on the bottom side of the upper substrate. The radiating patch is excited by a microstrip line which is printed on the top side of the lower substrate. To provide wide impedance matching bandwidth, a ground plane of microstrip feed line (the bottom side of the lower substrate) is defected by a dumbbell-shaped slot. Also, a metallic plate located at a distance of h_r from the lower substrate acts as a reflector to cancel the radiation along the backward direction and consequently improve F/B.

To design of the RSSFIP antenna, the important parameters that affect its performance are: substrate thickness (h_{ls}, h_{us}), substrate dielectric constant, distance between reflector and ground plane (h_r), patch dimensions, foam thickness (h_a), slot dimensions, and length of the open circuit stub (l_f). Due to the presence of Rogers RO4003C with thickness of 20 mil for construction, the thickness of the substrates is considered to be 0.508 mm and dielectric constant 3.55. Considering the central frequency of 10 GHz, the value $h_r = 7.5$ mm is considered.

A simple microstrip patch antenna is known as the basis of the RSSFIP antenna. The basic formulas for determining the length and width of a microstrip patch antenna are used. These formulas are [30]:

$$W_p = \frac{c}{2f_r}\sqrt{\frac{2}{\varepsilon_r + 1}} \tag{1}$$

$$\varepsilon_{eff} = \frac{\varepsilon_r + 1}{2} + \frac{\varepsilon_r - 1}{2}\left(\frac{2}{\sqrt{1 + 12h_{us}/W_p}}\right) \tag{2}$$

$$\Delta L_p = 0.712h_{us}\frac{(\varepsilon_{eff} + 0.3)\left[\dfrac{W_p}{h_{us}} + 0.264\right]}{(\varepsilon_{eff} - 0.258)\left[\dfrac{W_p}{h_{us}} + 0.813\right]} \tag{3}$$

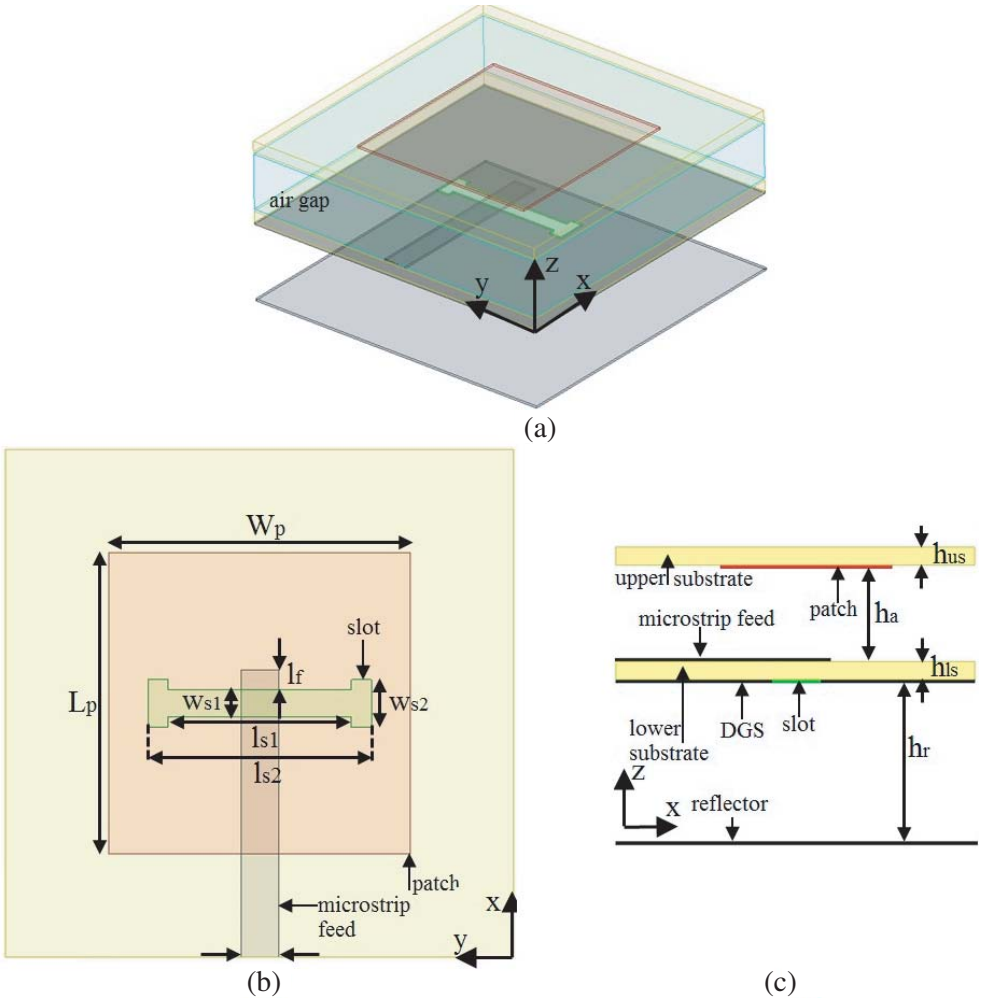

Figure 1. Geometry of the single antenna element (a) 3-D view (b) top view (c) side view.

$$L_p = \frac{c}{2f_r\sqrt{\varepsilon_{eff}}} - 2\Delta L_p \tag{4}$$

where W_p (width patch), L_p (length patch), and h_{us} (thickness upper substrate) are determined in Fig. 1. ΔL_p is the length reduced from the antenna to reduce fringing effects, ε_r the dielectric constant, c the speed of wave in free space, and ε_{eff} the effective dielectric constant. Using Eqs. (1)–(4), the patch antenna is designed using the following parameters: $\varepsilon_r = 3.55$, $h_{us} = 0.508$, $f_r = 10\,\text{GHz}$. The dimensions of the patch are calculated to be $L_p = 7.24\,\text{mm}$, $W_p = 9.94\,\text{mm}$.

The slot length is considered approximately 0.2λ [31]. The ratio of slot width to length is typically 1/10 [32]. For improving F/B and coupling, a slot at the end of the rectangular aperture (i.e., the H-shaped slot) is added [32]. These parameter values will be used later as the starting point to design various RSSFIP antennas considered in this work. The other two parameters (l_f and h_a) are obtained by using structure optimization with the aim of increasing impedance bandwidth.

CST Microwave Studio, based on the finite integration technique (FIT), was used to optimize and match the antenna to a $50\,\Omega$ line to resonate at 10 GHz. Detailed dimensions of the proposed antenna with linear array are listed in Table 1 after optimization. The simulated return loss of the RSSFIP antenna is shown in Fig. 2. The bandwidth of the single element is 17.5% from 8.9 GHz to 10.6 GHz with $S_{11} < -10\,\text{dB}$. The simulated H-plane and E-plane radiation patterns at 10 GHz for the RSSFIP antenna are shown in Fig. 3. The maximum gain for the single element is 9.74 dBi which is improved in comparison to conventional microstrip antennas. The gain of a conventional patch antenna is around 5 to 6 dBi [33, 34]. The cross polarization (x-pol.) for the antenna is less than $-33.7\,\text{dB}$ for the E-plane.

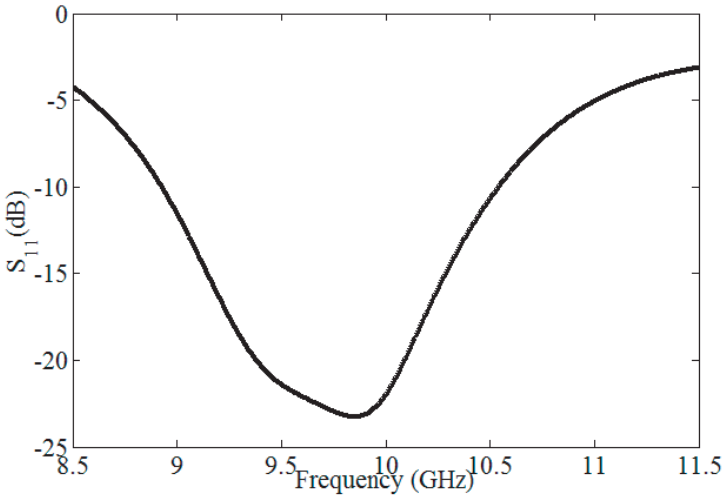

Figure 2. Return loss of the proposed RSSFIP antenna.

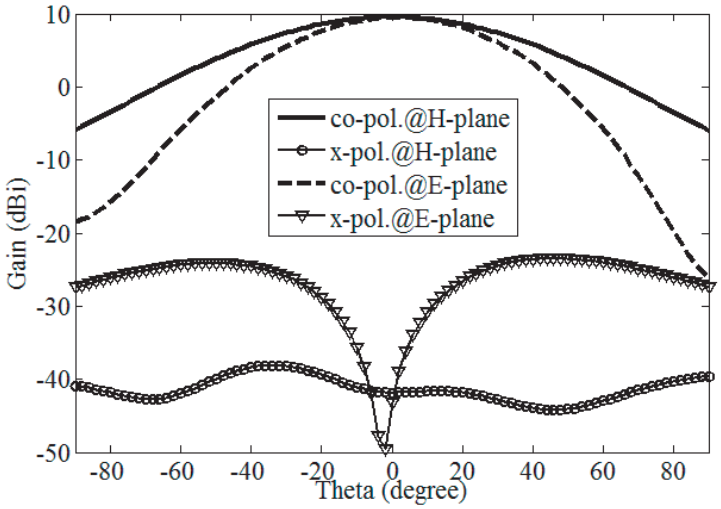

Figure 3. Radiation pattern of the proposed RSSFIP antenna at H-plane and E-plane for $f = 10\,\text{GHz}$.

2.2. Power Divider and Linear Array Design

The aim of this paper is to design a highly efficient and wideband phase array antenna with low SLL at H-plane; therefore, a conventional series-fed microstrip array antenna has to be designed. In addition, the use of series-fed arrays leads to a low SLL compared to the parallel fed array antenna. This is referred to as a linear array antenna. To increase the bandwidth of the array antenna, some alterations on this linear array antenna can be done. The linear array antenna is shown in Fig. 4. The linear array contains 16 RSSIP antennas presented at Section 2.1.

The linear array operates at 10 GHz and is designed for radiation in the broadside direction. The array is split into two linear subarrays and fed in the middle by the coaxial to microstrip line. This symmetric arrangement prevents the beam-pointing direction from varying with frequency. To guarantee an identical phase between the patches and to prepare a broadside radiation pattern, the distance between the feed points of the array patches should be arranged at one guided wavelength (λ_g). Because a single element is fed by a $50\,\Omega$ line, a quarter wavelength impedance transformer $70.71\,\Omega$ is required to convert it to a $100\,\Omega$ line. Next, due to the parallelism of the $50\,\Omega$ and $100\,\Omega$ lines, their equivalent impedance becomes $33.3\,\Omega$. As a result, to convert $33.3\,\Omega$ impedance to 100 ohms, the

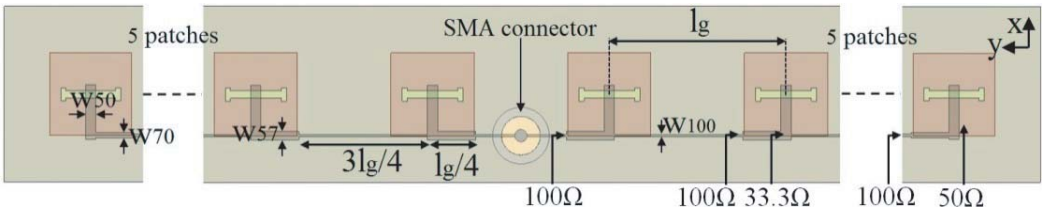

Figure 4. Schematic of the linear array antenna.

57.73 Ω impedance converter is required. This process continues until the coaxial port. In the end, it looks like two parallel 100 Ω lines connected to the coaxial port, creating the conditions for impedance matching. As a result, at the feeding line, two different quarter wavelength transformers (70.71 and 57.73 Ω) are used to build the proposed feeding network. The characteristics of these lines are listed in Table 1. The line numbers written in Table 1 match those displayed in Fig. 4. The inter-element spacing of 18.8 mm is adjusted such that all elements are excited in-phase.

Table 1. Detail dimensions of the proposed linear array antenna.

Parameter	Value (mm)	Parameter	Value (mm)
L_p	8.9	h_a	2.6
W_p	8.9	h_{us}	0.508
w_f	1.1	h_{ls}	0.508
l_f	0.6	l_g	18.8
w_{s1}	0.8	w_{50}	1.1
w_{s2}	1.4	w_{70}	0.6
l_{s1}	5.4	w_{57}	0.9
l_{s2}	6.6	w_{100}	0.3
h_r	7.5		

2.3. Full Array Design

Figure 5 shows the simulated $12 * 16$ microstrip array antenna, with an aperture size of $252 * 300.8\,\text{mm}^2$, constructed by using 12 linear arrays presented at Section 2.2. To scan the capability of the array antenna along the x-axis (E-plane), each linear array is fed separately. To increase the isolation between the linear arrays, a long rectangular defect is created on the ground plate. The distance between adjacent linear arrays is 21 mm. Using this feed topology for the array reduces the losses of the feed network. Therefore, this feed structure, in comparison to conventional ones, improves the radiation efficiency, gain-bandwidth performance, and wideband impedance matching of the array.

3. SIMULATION AND EXPERIMENTAL RESULTS

The fabricated microstrip array antenna is shown in Fig. 6. For the test of this array, Wilkinson divider 1 to 12 was used. Fig. 7 shows that the measured return loss is in good agreement with the simulated one but with a detailed change. The bandwidth of the array antenna is 24% and is from 8.8 GHz to 11.2 GHz with $S_{11} < -10$ dB. In addition, in this figure, the measured isolation between ports 1–2 and ports 1–3 is shown, indicating good isolation between the ports ($S_{21} < -25$ dB, $S_{31} < -37$ dB). Fig. 8 shows the measurement and simulation results of the radiation patterns at $f = 10$ GHz in the E plane and H plane. The half-power beamwidths of the E-plane and H-plane are close to 6° and 7.3°, respectively. The measured gain of the array antenna at $f = 10$ GHz is 28.5 dB for the E-plane

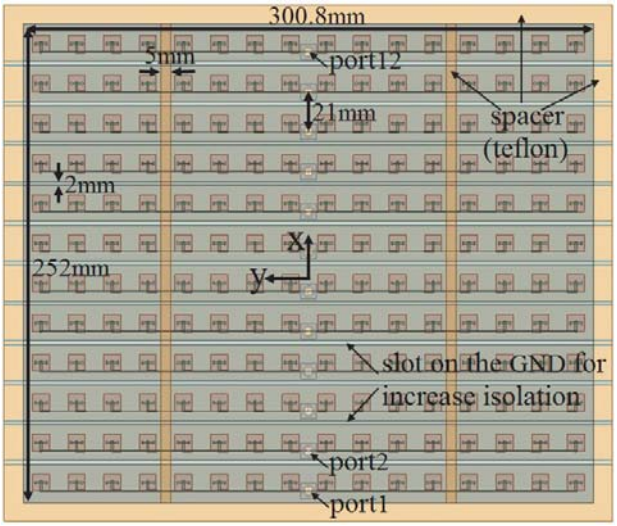

Figure 5. Schematic of the full microstrip array antenna.

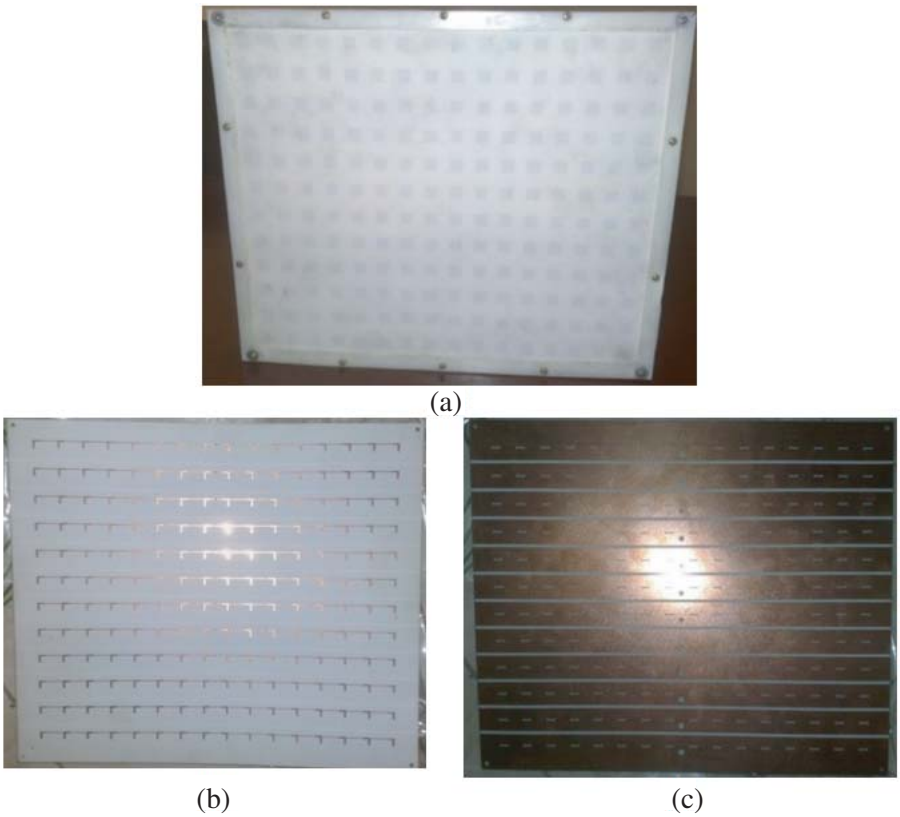

Figure 6. Photograph of the fabricated full array antenna. (a) Front view (b) feed network plane (c) ground plane with DGS.

and H-plane. Fig. 8(b) shows an SLL less than -24.5 dB and a cross-polarization less than -23.9 dB, indicating the good performance of this array antenna for military uses. The measured far field H-plane radiation patterns at two different frequencies over the bandwidth are shown in Fig. 9. Fig. 10 shows the measured gain of the proposed array antenna for various frequencies.

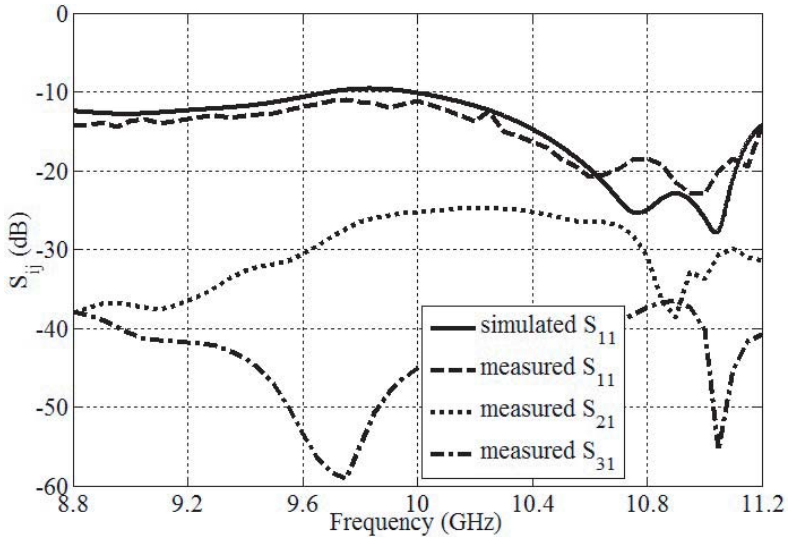

Figure 7. Simulated and measured return loss of the full array antenna with combiner and measured S_{21}, S_{31} without combiner.

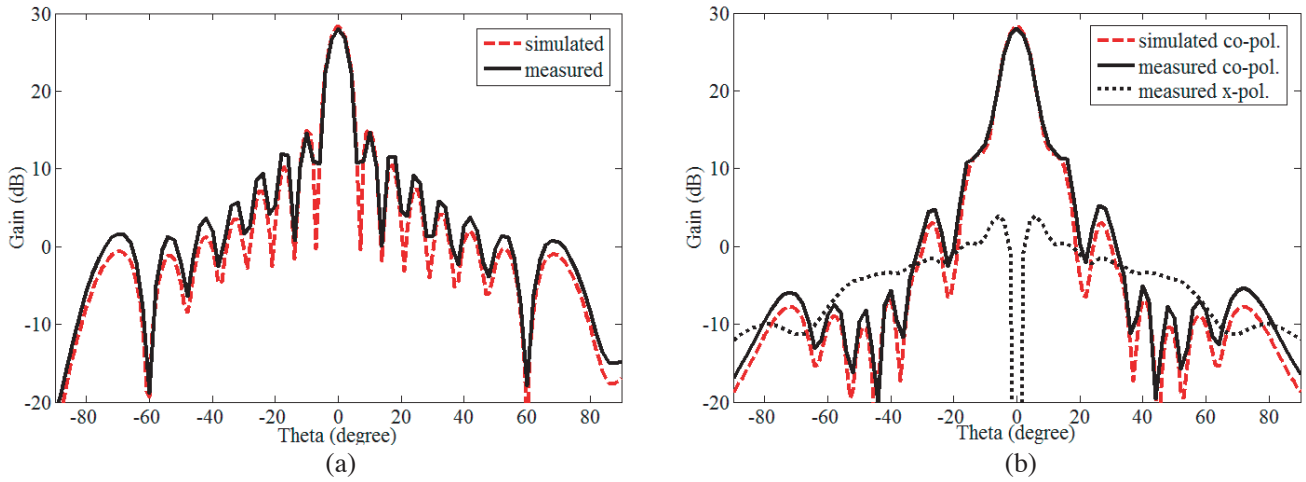

Figure 8. The radiation pattern and measured maximum gain of the full array antenna (a) E-plane radiation pattern at 10 GHz (b) H-plane radiation pattern at 10 GHz.

The measured gain in the main (zero) degree beam is 28.5 dB, and the physical aperture area of the antenna is $252 * 300.8\,\text{mm}^2$ without considering the spacer at the edges. The efficiency of the antenna can be derived from the relation [35]:

$$G = \frac{4\pi}{\lambda^2} A\eta_a \tag{5}$$

where G is the gain, η_a the efficiency of the antenna, A the physical aperture area, and λ the wavelength. Solving Eq. (5) with respect to η_a and inserting numerical values yield the result $\eta_a = 67\%$. Ordinarily, the efficiency of the microstrip array antenna is not more than 50%, using this method (series-fed and RFSSIP antenna) can considerably increase the efficiency of the antenna.

Table 2 presents an analogy between the measurement results of the proposed array antenna and some antennas fabricated. Remarkably, our fabricated array antenna has the widest bandwidth and highest efficiency between the mentioned antennas in Table 2.

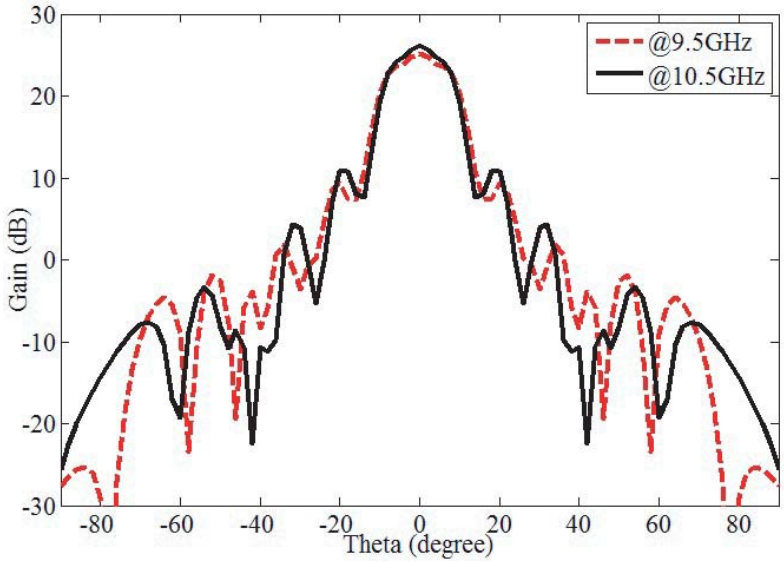

Figure 9. Measured H-plane radiation characteristics of the full array antenna at $f = 9.5,\ 10.5\,\text{GHz}$.

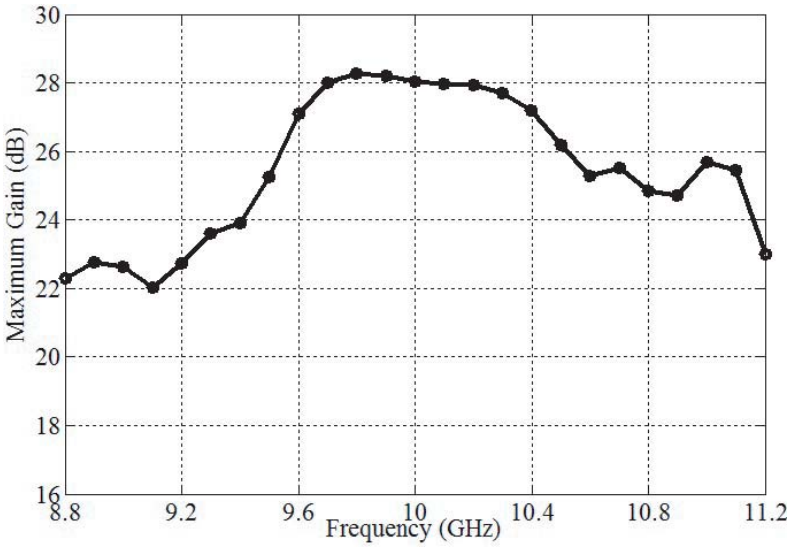

Figure 10. Measured maximum gain of the full array antenna.

Table 2. Comparison of the suggested array antenna with a few reported array antenna.

Ref	Freq (GHz)	Array size (λ_0^2)	Gain (dB)	Impedance BW	Aperture efficiency
[36]	5.76	3.15	12.8	2%	48%
[37]	59	1612	39.2	14.6%	41%
[38]	5.8	22.1	22.4	1.4%	60%
This work	**10**	**84.2**	**28.5**	**24%**	**67%**

4. CONCLUSION

This paper details a design procedure for high efficiency X-band series-fed microstrip array antenna for phase array applications. First, the RSSFIP antenna is designed. Then the series-fed linear array fed from the middle is studied and designed. At the end, the full array antenna for phased array applications is designed. The proposed $16 * 12$ array has a measured gain of 28.5 dB, 67% efficiency, and the XP of -23.9 dB at 10 GHz with an impedance bandwidth of 24%. The 3 dB gain bandwidth of the proposed antenna is 15.5% for SLL < -14 dB and 6% for SLL < -25 dB at H-plane. Due to the simulated and measured optimum results of the array antenna, this antenna is suitable for synthetic aperture radar (SAR) antenna and phased array applications.

REFERENCES

1. Bhattacharyya, A., D. Yang, and S. Nam, "Microstrip array antenna bandwidth enhancement using reactive surface," *Microw. Opt. Technol. Lett.*, Vol. 62, 825–829, 2020, https://doi.org/10.1002/mop.32081.
2. Kan, G., W. Lin, C. Liu, and D. Zou, "An array antenna based on coplanar parasitic patch structure," *Microw. Opt. Technol. Lett.*, Vol. 60, 1016–1023, 2018, https://doi.org/10.1002/mop.31104.
3. Jalali, M., M. Naser-Moghadasi, and R. A. Sadeghzadeh, "Quasi-self-complementary planar broadband series-fed array antenna for C-band applications," *Microw. Opt. Technol. Lett.*, Vol. 59, 95–98, 2017, doi:10.1002/mop.30228.
4. Wadkar, S., B. Hogade, R. Chopra, and G. Kumar, "Broadband and high gain stacked microstrip antenna array," *Microw. Opt. Technol. Lett.*, Vol. 61, 1882–1888, 2019, https://doi.org/10.1002/mop.31813.
5. Rabbani, M. and H. Ghafouri-Shiraz, "High gain microstrip antenna array for 60 GHz band point to point WLAN/WPAN communications," *Microw. Opt. Technol. Lett.*, Vol. 59, 511–514, 2017, doi:10.1002/mop.30332.
6. Chopra, R. and G. Kumar, "Series-fed binomial microstrip arrays for extremely low sidelobe level," *IEEE Trans. Antennas Propag.*, Vol. 67, 4275–4279, 2019.
7. Yang, G., J. Li, D. Wei, and R. Xu, "Study on wide-angle scanning linear phased array antenna," *IEEE Trans. Antennas Propag.*, Vol. 66, 450–455, 2018.
8. Li, M. and K.-M. Luk, "Low-cost wideband microstrip antenna array for 60- GHz applications," *IEEE Trans. Antennas Propag.*, Vol. 64, 3012–3018, 2014.
9. Shen, X., Y. Liu, L. Zhao, G. Huang, X. Shi, and Q. Huang, "A miniaturized microstrip antenna array at 5G millimeter-wave band," *IEEE Antennas Wireless Propag. Lett.*, Vol. 18, 1671–1675, 2019.
10. James, J. R., P. S. Hall, and C. Wood, "Microstrip antenna theory and design," Ch. 5, 6, London, UK, Peregrinus, 1981.
11. Mailloux, R. J., J. F. Mcilvenna, and N. P. Kernweis, "Microstrip array technology," *IEEE Trans. Antennas Propag.*, Vol. 29, 25–37, 1981.
12. Yin, J., Q. Wu, C. Yu, H. Wang, and W. Hong, "Low-sidelobe-level series-fed microstrip antenna array of unequal interelement spacing," *IEEE Antennas Wireless Propag. Lett.*, Vol. 16, 1695–1698, 2017.
13. Mohamed, I. and A. R. Sebak, "High-gain series-fed aperture-coupled microstrip antenna array," *Microw. Opt. Technol. Lett.*, Vol. 57, 91–94, 2015, doi:10.1002/mop.28792.
14. Ku, C.-H., H.-W. Liu, and Y.-S. Lin, "Novel series-fed microstrip array antenna with miniaturized feeding network for WLAN/RFID applications," *Microw. Opt. Technol. Lett.*, Vol. 53, 1727–1730, 2011, doi:10.1002/mop.26120.
15. Soliman, E. A., A. Vasylchenko, V. Volski, W. De Raedt, and G. A. E. Vandenbosch, "Sixteen-by-sixteen array of series-fed aperture-coupled microstrip patch antennas," *Microw. Opt. Technol. Lett.*, Vol. 53, 2705–2711, 2011, doi:10.1002/mop.26310.

16. Yeo, J. and J.-I. Lee, "Broadband compact series-fed dipole pair antenna with simplified integrated balun," *Microw. Opt. Technol. Lett.*, Vol. 56, 1731–1734, 2014, doi:10.1002/mop.28432.
17. Jalali, M., M. Naser-Moghadasi, and R. A. Sadeghzadeh, "Quasi-self-complementary planar broadband series-fed array antenna for C-band applications," *Microw. Opt. Technol. Lett.*, Vol. 59, 95–98, 2017, doi:10.1002/mop.30228.
18. Im, Y.-T., J.-H. Lee, Y.-W. Jeong, L. Sang-Ik, and S.-O. Park, "A polarization selective series-fed array antenna," *Microw. Opt. Technol. Lett.*, Vol. 52, 1861–1864, 2010, doi:10.1002/mop.25323.
19. Karimkashi, S. and G. Zhang, "A dual-polarized series-fed microstrip antenna array with very high polarization purity for weather measurements," *IEEE Trans. Antennas Propag.*, Vol. 61, 5315–5319, 2013.
20. Alibakhshikenari, M., B. S. Virdee, and E. Limiti, "Study on isolation and radiation behaviours of a 34×34 array-antennas based on SIW and metasurface properties for applications in terahertz band over 125–300 GHz," *Optik*, Vol. 206, 1–10, 2020.
21. Alibakhshikenari, M., B. S. Virdee, N. Ojaroudi, P. Shukla, K. Quazzane, C. H. See, R. Abd-Alhameed, F. Falcone, and E. Limiti, "Isolation enhancement of densely packed array antennas with periodic MTM-photonic bandgap for SAR and MIMO systems," *IET Microw. Antennas Propag.*, 1–8, 2019.
22. Alibakhshikenari, M., B. S. Virdee, C. H. See, R. A. Abd-Alhameed, F. Falcone, and E. Limiti, "High-isolation leaky-wave array antenna based on CRLH-metamaterial implemented on SIW with $\pm 30^\circ$ frequency beam-scanning capability at millimetre-waves," *Electronics*, Vol. 8, 1–15, 2019.
23. Alibakhshikenari, M., M. Khalily, B. S. Virdee, C. H. See, R. A. Alhameed, and L. Limiti, "Mutual-coupling isolation using embedded metamaterial EM bandgap decoupling slab for densely packed array antennas," *IEEE Access*, Vol. 7, 51827–51840, 2019.
24. Alibakhshikenari, M., M. Khalily, B. S. Virdee, C. H. See, R. A. Abd-Alhameed, E. Limiti, "Mutual coupling suppression between two closely placed microstrip patches using EM-bandgap metamaterial fractal loading," *IEEE Access*, Vol. 7, 23606–23614, 2019.
25. Alibakhshikenari, M., B. S. Virdee, C. H. See, R. A. Abd-Alhameed, A. H. Ali, F. Falcone, and E. Limiti, "Study on isolation improvement between closely-packed patch antenna arrays based on fractal metamaterial electromagnetic bandgap structures," *IET Microw. Antennas Propag.*, Vol. 11, 2241–2247, 2018.
26. Alibakhshikenari, M., B. S. Virdee, and C. H. See, R. A. Abd-Alhameed, F. Falcone, and E. Limiti, "Surface wave reduction in antenna arrays using metasurface inclusion for MIMO and SAR systems," *Radio Science*, Vol. 54, 1067–1075, 2019.
27. Alibakhshikenari, M., B. S. Virdee, P. Shukla, C. H. See, R. A. Abd-Alhameed, M. Khalili, F. Falcone, and E. Limiti, "Interaction between closely packed array antenna elements using meta-surface for applications such as MIMO systems and synthetic aperture radars," *Radio Science*, Vol. 53, 1368-1381, 2018.
28. Alibakhshikenari, M., C. H. See, B. S. Virdee, and R. A. Abd-Alhameed, "Meta-surface wall suppression of mutual coupling between microstrip patch antenna arrays for THz-band applications," *Progress In Electromagnetics Research Letters*, Vol. 75, 105–111, 2018.
29. Alibakhshikenari, M., B. S. Virdee, P. Shukla, C. H. See, R. Abd-Alhameed, M. Khalily, F. Falcone, and E. Limiti, "Antenna mutual coupling suppression over wideband using embedded periphery slot for antenna arrays," *Electronics*, Vol. 7, 1–11, 2018.
30. Balanis, C. A., *Antenna Theory: Analysis and Design*, 4th Edition, Wiley, Hoboken, NJ, 2016.
31. Civerolo, M. and D. Arakaki, "Aperture coupled patch antenna design methods," *IEEE International Symposium on Antennas and Propagation (APSURSI)*, 876–879, Spokane, WA, 2011.
32. Zarreen, A. and S. C. Shrivastava, "An introduction of aperture coupled microstrip slot antenna," *International Journal of Engineering Science and Technology*, Vol. 2, 36–39, 2010.
33. Li, X., J. Li, J. Tang, X. Wu, and Z. Zhang, "High gain microstrip antenna design by using FSS superstrate layer," *4th International Conference on Computer Science and Network Technology (ICCSNT)*, 1186–1189, Harbin, 2015.

34. Kharade A. R. and V. P. Patil, "Enhancement of gain of rectangular microstrip antenna using multilayer multidielectric structure," *IOSR Journal of Electronics and Communication Engineering*, Vol. 2, 35–40, 2012.
35. Wu, W., J. Yin, and N. Yuan, "Design of an efficient X-band waveguide-fed microstrip patch array," *IEEE Trans. Antennas Propag.*, Vol. 55, 1933–1939, 2007.
36. Chopra, R. and G. Kumar, "Series-fed binomial microstrip arrays for extremely low sidelobe level," *IEEE Trans. Antennas Propag.*, Vol. 67, No. 6, 4275–4279, 2019.
37. Wu, J., Y. J. Cheng, and Y. Fan, "A wideband high-gain high-efficiency hybrid integrated plate array antenna for V-band inter-satellite links," *IEEE Trans. Antennas Propag.*, Vol. 63, 1225–1233, 2015.
38. Chopra, R. and G. Kumar, "Series- and corner-fed planar microstrip antenna arrays," *IEEE Trans. Antennas Propag.*, Vol. 67, 5982–5990, 2019.